

Tilted fiber Bragg grating based optical sensor for simultaneous measurement of vital signs: a novel approach

Ramya Arumugam, Ramamoorthy Kumar, Samiappan Dhanalakshmi

Department of Electronics and Communication Engineering, College of Engineering and Technology, SRM Institute of Science and Technology, Chengalpattu, India

Article Info

Article history:

Received Jul 2, 2024

Revised Sep 2, 2024

Accepted Oct 1, 2024

Keywords:

Optical sensor

Tilted fiber Bragg grating

Simultaneous measurement

Temperature

Heart rate

Vital sign

ABSTRACT

Vital signal monitoring acts as a highly significant diagnostic method. Continuous monitoring of vital signs like temperature, heart rate, and blood pressure aids in easy and fast disease diagnosis. Existing methods that enable continuous monitoring, such as smart watches, are not accurate enough to be used as a benchmark for diagnosing diseases. In this paper, we propose simultaneous temperature and heart rate measurement using tilted fiber Bragg grating (TFBG) which enables concurrent measurement of measurands due to its intrinsic optical property. Temperature and heart rate were considered for measurement. The proposed TFBG-based optical sensor has a sensitivity of 11.81 pm/°C and 1.73 pm/με towards variation in temperature and strain, respectively. The sensitivity was determined by a shift in the wavelength of core mode resonance for temperature and a differential change in the wavelength of cladding mode resonance for heart rate. The average response time of the proposed TFBG sensor was found to be 3 seconds. Accuracy of 99.68% and 98.42% were achieved in temperature and heart rate measurements by the proposed TFBG sensor. The acceptability of the proposed TFBG sensor was analyzed using the Bland-Altman plot.

This is an open access article under the [CC BY-SA](https://creativecommons.org/licenses/by-sa/4.0/) license.



Corresponding Author:

Ramamoorthy Kumar

Department of Electronics and Communication Engineering, College of Engineering and Technology,

SRM Institute of Science and Technology

Kattankulathur, Chengalpattu 603203, India

Email: kumarr@srmist.edu.in

1. INTRODUCTION

The evolution of fiber Bragg grating (FBG) based optical sensors in biomedical applications and clinical practices is undeniable. This growth is due to the main aspect that these optical sensors are immune to interference from electromagnetic waves, have high sensitivity and accuracy in addition to having other advantages such as flexibility, versatility, fast response time, compact size, remote sensing, and reliability [1], [2]. The ascendancy of FBG finds its application in various fields such as temperature and strain sensing, multiplexers, lasers, in the medical field, structural health monitoring, and corrosion monitoring [3]–[9]. In the medical field, it is widely used to monitor vital signs. Several recent studies [10]–[16] have suggested that shows the implementation of FBG in measuring body temperature and heart rate or respiration rate. Nedoma *et al.* [10] implements FBG for heart rate, respiration rate, and body temperature using two FBG sensors encapsulated in polydimethylsiloxane polymer (PDMS) material that exhibits a total relative error of 0.31%. Two FBGs were used to assess the body temperature and heart rate of 128 individuals, and the measured value lies within the ± 1.96 deviation range [11]. Manujlo and Osuch [12] discussed the implementation of FBG to measure respiration rate using exhaled air temperature and compares the readings with electronic

sensors and portrait the advantage of the ability to measure fast and slow breathing. Body temperature using FBG for the range of 35 °C to 41 °C was implemented and sensitivity and resolution of 85.9% was achieved in [13], [14] proposes implementing FBG sensors for temperature monitoring with the aid of integration into hardware made of polylactic acid (PLA) device with a thin layer of copper encapsulation that enhances the wavelength shift. Chethana *et al.* [15] implements a FBG heartbeat device to simultaneously monitor cardiac and respiratory activities and additionally sensing heartbeat rhythm, monitoring cardiac activity, heart rate variability, and breathing activity. FBG encapsulated in fiberglass was used in an magnetic resonance imaging (MRI) environment to calculate respiration rate and heart rate [16] continuously. It was observed that within the ± 1.96 deviation range lies 95.36% samples for the respiration rate and 95.13% samples for the heart rate with a relative error below 5%. Nedoma *et al.* [17] proposes a polydimethylsiloxane (PDMS) encapsulated FBG for monitoring respiratory rate and heart rate from the movement of the thoracic cavity. Krej *et al.* [18] proposes a digital signal processing technique to measure heart rate and optimize it using a genetic algorithm. Kurasawa *et al.* [19] implements a FBG sensor to calculate glucose level from pulse wave measured at radial artery. The above-referred works use FBG for single parameter measuring or multiple FBG sensors for simultaneous measurement of parameters. Further advancements are carried out by introducing polymer fiber [20], helical fiber [21], smart textiles with sensor embedded [22], [23], proposing new apodization functions [24], [25], using hetero core fiber [26], using four core fiber [27], using partially coated fiber [28], using no core fiber [29], using two-level encapsulations in Teflon pipe and capillary tube [30], using Bragg fibers [31].

In this work, we propose a tilted fiber Bragg grating (TFBG) based optical sensor to overcome the disadvantage of cross-sensitivity and need for additional modification for simultaneous measurement of multiple parameters. The tilt in the grating structure enables core and cladding mode resonances [32]. The differential responsiveness of core and cladding resonances [33], allows the possibility of measuring different measurands simultaneously. An experimental investigation was carried out to calibrate and validate the proposed sensor for simultaneous monitoring of vital signs such as body temperature and heart rate. Table 1 provides the state of the art for this study.

The structuring of the current work is as section 2 gives details of the structure of TFBG and its sensing principle. Section 3 elaborates on the setup for the experimental investigation of the proposed TFBG. Section 4 presents the results and its discussion. Finally, section 5 encapsulates the conclusion, followed subsequently by references.

Table 1. State-of-the-art comparison

Sensor type	Sensor position	Measured parameters	Sensitivity/error (%)	Reference
2 FBG with PDMS	Chest	Body temperature, heart rate, respiration rate	0.010 nm/°C, ± 1.96 range for heart rate	[11]
2 FBG with PDMS	Chest wall, thorax	Body temperature, heart rate	0.31 nm/°C, ± 1.96 range for heart rate	[17]
Polymer FBG	Chest	Body temperature, heart rate	-0.055 nm/°C, $\pm 2\%$ for heart rate	[20]
FBG with fiber glass	Thorax	Heart rate, respiration rate	11.3 nm/°C, 4.87% for heart rate	[21]
FBG	Thorax and neck	Heart rate, respiration rate	2% error for heart rate	[22]
Proposed TFBG	Wrist	Body temperature, heart rate	0.0112 nm/°C, ± 1.96 range for heart rate	-

2. PRINCIPLE OF TILTED FIBER BRAGG GRATING

2.1. Theoretical background of tilted fiber Bragg grating

In FBGs, the modulation in refractive index in the core region results in Bragg resonance due to coupling in the forward and backward propagating core modes. Bragg resonance is affected by both temperature and strain applied. Along with Bragg resonance, FBGs show many weak resonances in the transmission spectrum which results from coupling to cladding guided modes. These weak resonances are undetected in the reflection spectrum due to losses in power.

TFBGs vary from FBGs in the aspect that the grating fringes in the core region are tilted by an angle (θ) in accordance with the fiber axis. The tilt enhances cladding mode resonance by coupling a forward-propagating core mode and backward-propagating cladding mode. TFBG can be implemented for sensing many parameters by selecting which resonances give the best sensitivity for a given measurand. When the tilt angle increases, the coupled resonances shift towards shorter wavelengths. The structure of TFBG is shown in Figure 1.

Figure 2 shows the transmission spectra of TFBG. The core mode resonance is centered at the Bragg wavelength and the cladding mode spreads over a wide wavelength range consisting of many peaks. TFBG sensitivity depends on core mode and peak wavelengths in cladding mode. When temperature is applied, all

resonances have a global shift, enabling the TFBG to measure temperature without cross-sensitivity from other modalities. The relative shift in core and cladding resonances indicates change in applied temperature.

When axial strain is applied, the variation in the periodicity results in the modification of effective refractive indices. Resonances of cladding modes fall short of core mode resonance as the higher cladding modes have smaller indices compared to the core mode. Lag in the shift increases with increasing strain.

The equations (1)-(3) describe the principle of TFBG [34]. The TFBG grating period (Λ_g) is given as (1):

$$\Lambda_g = \Lambda / \cos\theta \tag{1}$$

where Λ is the grating period along the fiber axis and θ is the tilt angle in accordance with the fiber axis. The wavelength of core and i^{th} cladding mode resonances in the transmission spectrum of TFBG is given as,

$$\lambda_{\text{core}} = (2n_{\text{eff,core}} \Lambda) / \cos\theta \tag{2}$$

$$\lambda_{\text{clad}}^i = (n_{\text{eff,core}} + n_{\text{eff,clad}}^i) \Lambda / \cos\theta \tag{3}$$

where λ_{core} , λ_{clad}^i are the wavelength of core and i^{th} cladding mode respectively; $n_{\text{eff,core}}$, $n_{\text{eff,clad}}^i$ are the effective refractive index of the core and i^{th} cladding mode respectively.

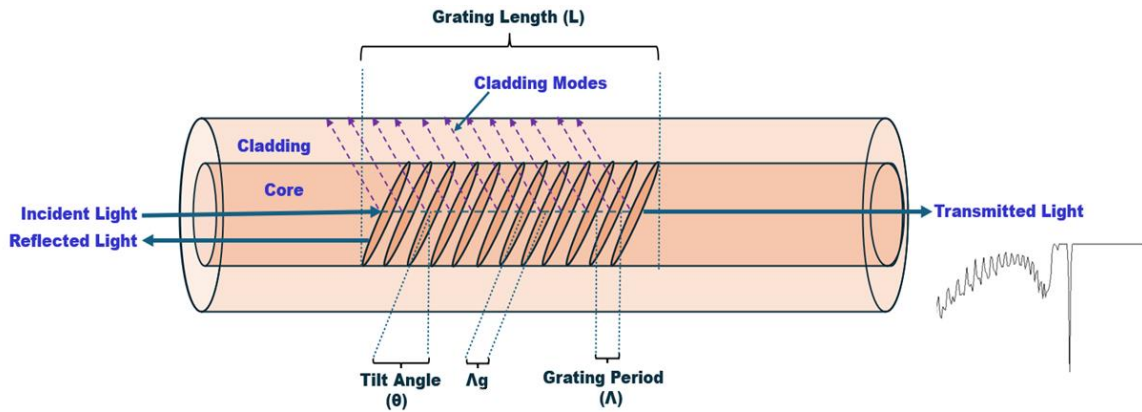


Figure 1. TFBG structure

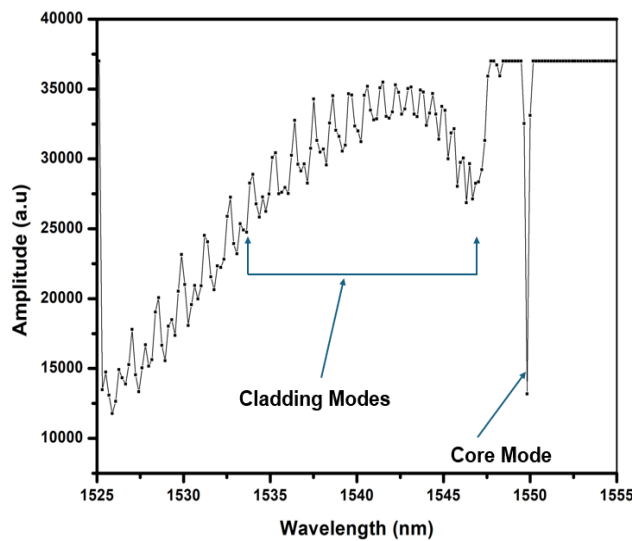


Figure 2. Transmission spectrum of TFBG

2.2. Sensitivity of TFBG

The sensing principle of TFBGs is analogous to FBGs. The wavelength of the core and cladding mode in the transmission spectrum will change according to the measurand applied. The tilt in the grating structure induces different sensitivity to strain and temperature. Wavelength shift in core and cladding mode resonances differs with temperature and strain, enabling simultaneous measurement of both. Equations (4) and (5), which define the shift in the core and its cladding mode, characterize temperature sensitivity [34].

$$\Delta\lambda_{core} = 2 \left(\frac{\Lambda}{\cos\theta} \frac{\partial n_{eff}}{\partial T} + \frac{n_{eff}}{\cos\theta} \frac{\partial \Lambda}{\partial T} \right) \Delta T = K_{core,T} \Delta T \quad (4)$$

$$\Delta\lambda_{clad}^i = \left(\frac{\Lambda}{\cos\theta} \frac{\partial (n_{eff,core}^i + n_{eff,clad}^i)}{\partial T} + \frac{(n_{eff,core}^i + n_{eff,clad}^i)}{\cos\theta} \frac{\partial \Lambda}{\partial T} \right) \Delta T = K_{clad,T}^i \Delta T \quad (5)$$

where $\Delta\lambda_{core}$ and $\Delta\lambda_{clad}^i$ are the change in wavelength in core and cladding resonances respectively. ΔT is the change in applied temperature.

The applied strain in the TFBG results in the elongation of the grating period and refractive index change. Equations (6) and (7) show how the strain sensitivity shifts the core and cladding resonances, respectively [34].

$$\Delta\lambda_{core} = 2 \left(\frac{\Lambda}{\cos\theta} \frac{\partial n_{eff}}{\partial \varepsilon} + \frac{n_{eff}}{\cos\theta} \frac{\partial \Lambda}{\partial \varepsilon} \right) \Delta \varepsilon = K_{core,\varepsilon} \Delta \varepsilon \quad (6)$$

$$\Delta\lambda_{clad}^i = \left(\frac{\Lambda}{\cos\theta} \frac{\partial (n_{eff,core}^i + n_{eff,clad}^i)}{\partial \varepsilon} + \frac{(n_{eff,core}^i + n_{eff,clad}^i)}{\cos\theta} \frac{\partial \Lambda}{\partial \varepsilon} \right) \Delta \varepsilon = K_{clad,\varepsilon}^i \Delta \varepsilon \quad (7)$$

where $\Delta \varepsilon$ is the change in applied strain. Equations (10) and (11) are obtained from (6) and (7) by considering the substitution of (8) and (9) in it.

$$p_{core} = -\frac{1}{n_{eff,core}} \frac{\partial n_{eff,core}}{\partial \varepsilon} \quad (8)$$

$$p_{clad}^i = -\frac{1}{(n_{eff,core}^i + n_{eff,clad}^i)} \frac{\partial (n_{eff,core}^i + n_{eff,clad}^i)}{\partial \varepsilon} \quad (9)$$

$$\Delta\lambda_{core} = \lambda_{core} (1 - p_{core}) \Delta \varepsilon \quad (10)$$

$$\Delta\lambda_{clad}^i = \lambda_{clad}^i (1 - p_{clad}^i) \Delta \varepsilon \quad (11)$$

The relation between wavelength shift and the applied temperature and strain for concurrent sensing is given as [34].

$$\begin{pmatrix} \Delta\lambda_{core} \\ \Delta\lambda_{clad}^i \end{pmatrix} = \begin{pmatrix} K_{core,\varepsilon} & K_{core,T} \\ K_{clad,\varepsilon}^i & K_{clad,T}^i \end{pmatrix} \begin{pmatrix} \Delta \varepsilon \\ \Delta T \end{pmatrix} \quad (12)$$

Equation (12) states that simultaneous measurement is feasible by the shift in core and cladding resonances.

3. EXPERIMENTAL SETUP

The experimental setup to ascertain the sensitivity of the proposed TFBG is carried out with an optical broadband source, proposed TFBG, an optical interrogator, and a testing chamber is shown in Figure 3. The optical source employed is DL-BX9-CS5153A with 1.92 mW input power. It emits light with a wavelength of 1,535 to 1,565 nm range. The interrogator (I-MON 256 USB) has a 1,525 to 1,570 nm detection range and a resolution of 0.3 pm. TFBG proposed is of model T75. The fabrication used is the phase mask method which is used for mass production of identical gratings. In this method, the inclination angle is inscribed by keeping the phase mask and fiber at 90° to the writing beam and spinning the phase mask. Table 2 provides the design specification of the proposed TFBG. The light emitted from the source is connected to the proposed TFBG. The transmission spectrum is observed for wavelength shift in the receiver end with an interrogator connected to a computer. Wavelength shift occurs in core and cladding resonances according to the sensing parameter. Strain is applied to the polyimide-coated proposed TFBG in the form of a change in humidity. Moisture absorption causes the coating to swell, generating a strain on the TFBG underneath. The relation between the strain on the fiber due to moisture absorption is given as (13).

$$\varepsilon_{pi} = \alpha_{pi} * \Delta H \quad (13)$$

where ε_{pi} is the generated strain, α_{pi} is the hygroscopic expansion coefficient of polyimide and ΔH is the humidity change applied.

Figure 4 shows the real time investigation of proposed TFBG for concurrent temperature and heart rate measurement with Figure 4(a) showing the test bench setup and Figure 4(b) showing the experimental setup. For validation of measured data, the reference temperature and heart rate were measured using a standard thermometer and heart rate monitor. The reference thermometer used for temperature measurement is the TG8818B infrared thermometer. The testing range of the thermometer is 0 to 3cm and the testing speed is 0.5 s. The accuracy is ± 0.3 °C and has a repeatability of ± 0.1 °C. The reference heart rate monitor used for pulse rate measurement is the Rite check blood pressure monitor. It measures pulse rate, diastolic and systolic blood pressure. The heart rate specifications are: Measurement mode is oscillographic testing mode, the measurement range is 40 to 199 beats/ minute and accuracy is $\pm 5\%$ of a pulse value.

Table 2. Parameters of proposed TFBG

Parameters	Specifications
Grating length	15 mm
Grating profile	Gaussian
Tilting angle	5°
Full width at half maximum (FWHM)	0.23 nm
Coating	Polyimide
Reflectivity	98.246%
Connector	Ferrule connector-angled physical contact (FC/APC)

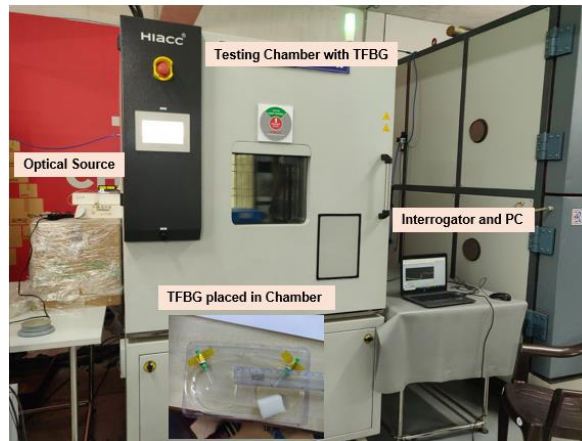


Figure 3. Experimental setup to investigate the sensitivity of TFBG for temperature and strain

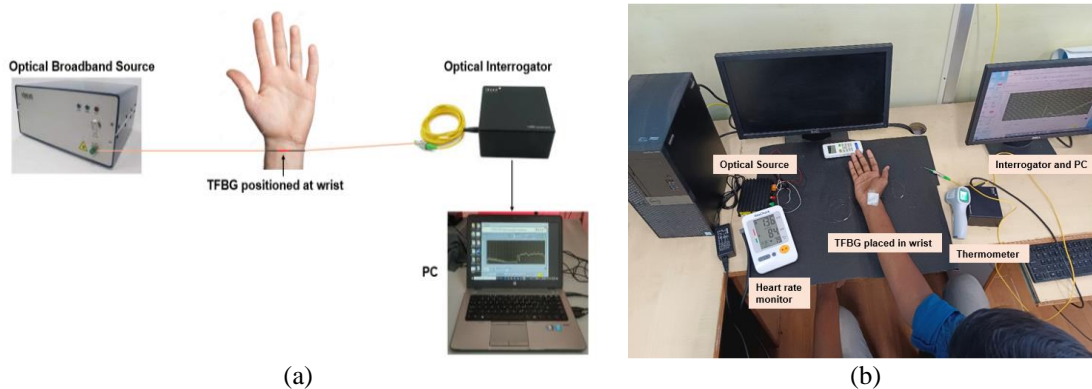


Figure 4. Real-time investigation of the sensitivity of TFBG for temperature and heart rate
(a) test bench setup and (b) experimental setup

4. RESULTS AND DISCUSSION

The sensitivity of the proposed TFBG to temperature and strain was determined by placing the fiber in the testing chamber and varying the parameters in a controlled environment. The temperature sensitivity was calculated by varying temperature with a constant strain (constant humidity) of $0\mu\epsilon$. Figure 5 shows the proposed TFBG's transmission spectrum for various temperature values. The core and cladding mode resonances show a wavelength shift of $11.81\text{ pm}/^\circ\text{C}$ at constant strain. Figure 6 shows the linearity in the wavelength shift for applied change in temperature in Figure 6(a) core mode resonance and Figure 6(b) cladding mode resonance. 14th cladding peak resonance is considered for investigating the wavelength shift. Strain sensitivity was determined by varying strain with constant temperature at 25°C . Figure 7 shows the proposed TFBG's transmission spectra for varying strain values. On observation, the core mode resonance shows a shift of $1.73\text{ pm}/\mu\epsilon$ at a constant temperature. The cladding modes show differential shifts in wavelength for varying strain. By analysis, it was found that the 14th peak cladding mode gave the maximum wavelength shift, and the same was considered for calculating strain. Lag was found in cladding mode resonance compared to core mode resonance for increasing strain. Figure 8 exhibits the linearity in the wavelength shift for applied strain variation in Figure 8(a) core mode resonance and Figure 8(b) 14th cladding mode resonance.

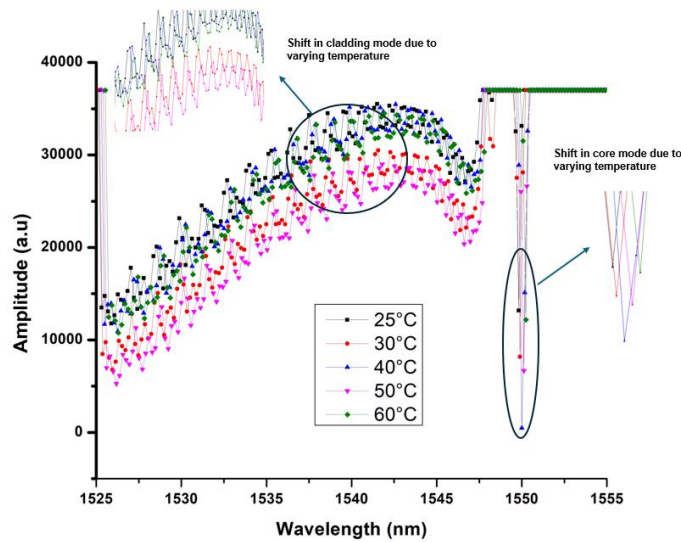


Figure 5. Transmission spectrum of proposed TFBG showing wavelength shift for varying temperature at constant strain

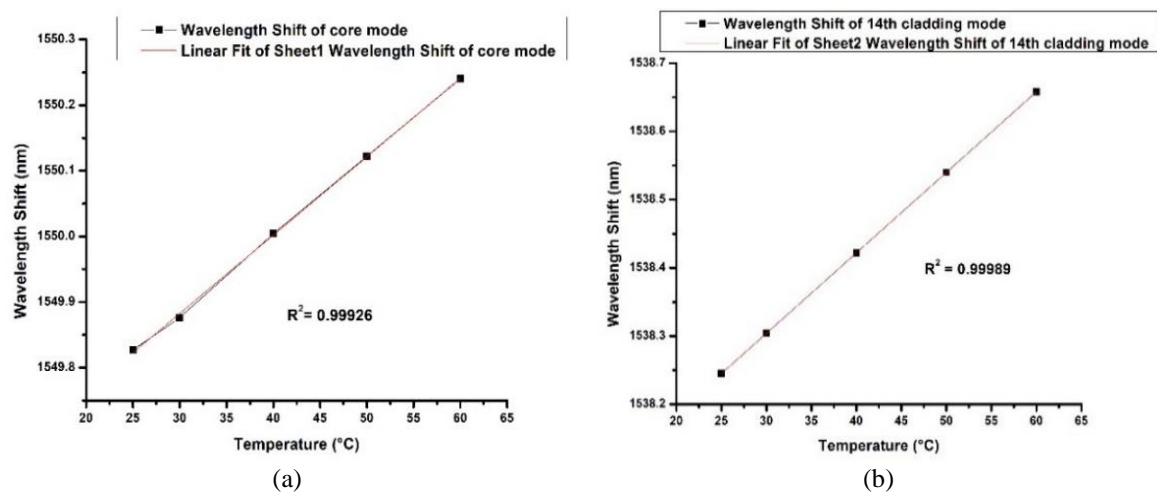


Figure 6. Linearity in wavelength shifts for (a) core and (b) cladding resonances for varying temperature at constant strain

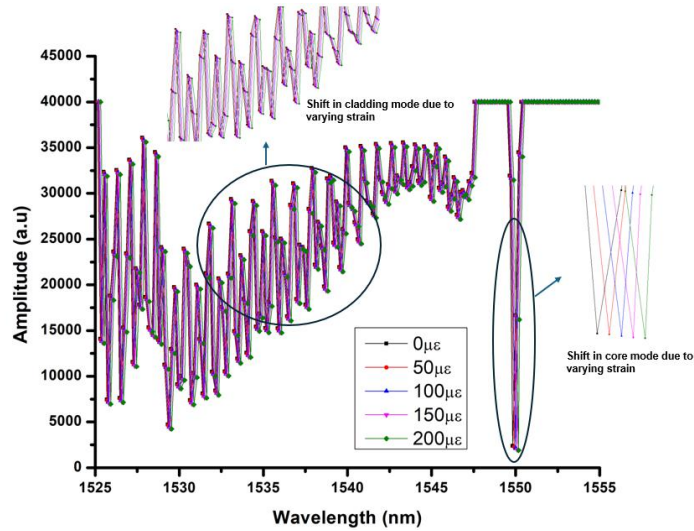


Figure 7. Transmission spectrum of proposed TFBR showing wavelength shift for varying strain at a constant temperature

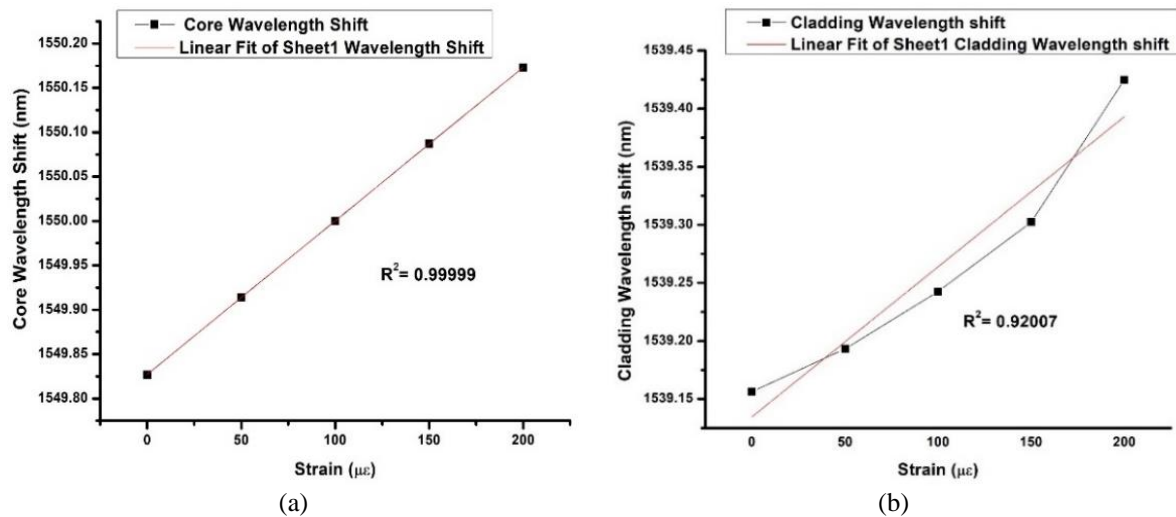


Figure 8. Linearity in wavelength shifts for (a) core and (b) cladding resonances for varying strain at constant temperature

The real-time investigation of simultaneous temperature and heart rate measurement was performed with the help of six volunteers (S1 to S6) (3 males and 3 females). The experiment was conducted in a controlled lab environment after getting consent from the six volunteers. The volunteers' ages range from 20 to 36, their height from 155 to 185 cm, and their weight from 60 to 85 kg. The proposed TFBR sensor was placed at the wrist position for all six volunteers and the reference measurement was done simultaneously in the same environment condition. Each volunteer was tested for 180 seconds and the same was repeated 3 times. The measurement was taken for 180 seconds and the value at the end of the measuring period was taken for validation. Figure 9 shows the transmission spectrum of the proposed TFBR for real time investigation. Figure 9(a) shows the transmission spectrum for all six volunteers and Figure 9(b) compares the spectrum of S1 and S4 for a better understanding of wavelength shift in resonances.

From the spectrum, it was determined that the core mode resonance exhibits a wavelength shift of $11.2 \text{ pm}/^\circ\text{C}$ for the temperature change. The varying heart rate was measured from the wavelength shift of the 14th cladding mode since it shows the maximum change for applied strain. The wavelength shift in core and cladding mode resonances for all six volunteers is shown in Figure 10. It was observed that, on average a heartbeat produces a wavelength shift of 28.62 pm in 14th peak cladding resonance.

Temperature was computed from the wavelength shift of core mode resonance and heart rate was calculated from the time interval between the peaks of the 14th cladding mode resonance. To estimate time intervals between peaks, a separate set of data was recorded for each volunteer for 10 s, which computed the intensity of the cladding peak against the timestamp. Figure 11 shows the number of peaks recorded for 6 seconds for volunteer S4 with normalized amplitude. S4 is shown for instance as heart rate for S4 volunteer is maximum among all volunteers (102 bpm).

The heart rate is calculated from the time interval between peaks as given [11].

$$\text{Heart rate} = \frac{60}{T_{avg}} \tag{14}$$

where T_{avg} is the average time interval between successive peaks.

$$T_{avg} = \frac{1}{n-1} \sum_{i=1}^{n-1} t_{i+1} - t_i \tag{15}$$

where n is the number of peaks and $t_{i+1} - t_i$ gives the time interval between successive peaks.

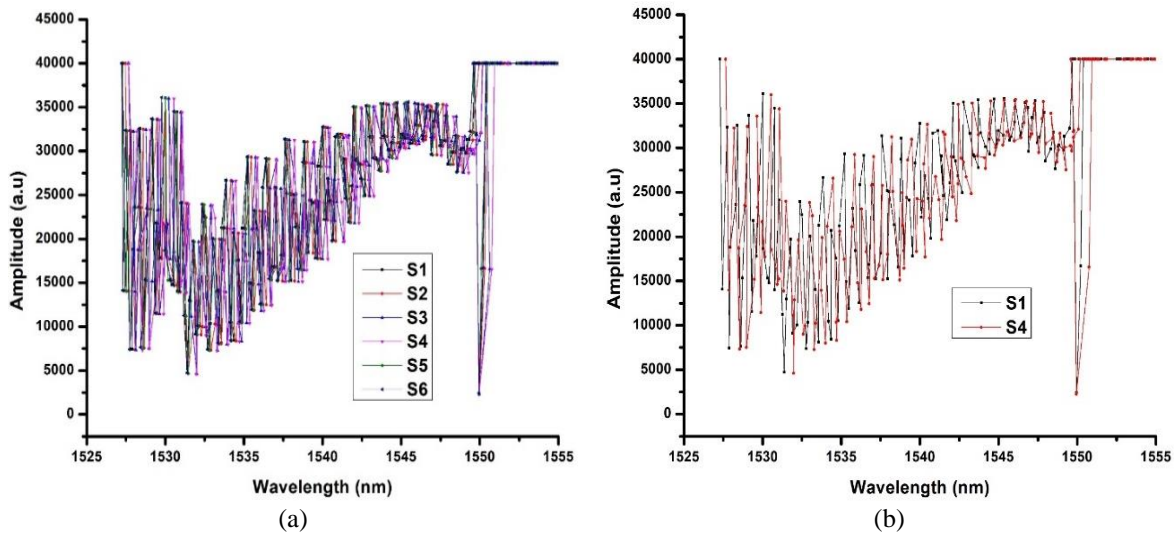


Figure 9. Transmission spectrum of proposed TFBG for (a) six volunteers and (b) two volunteers

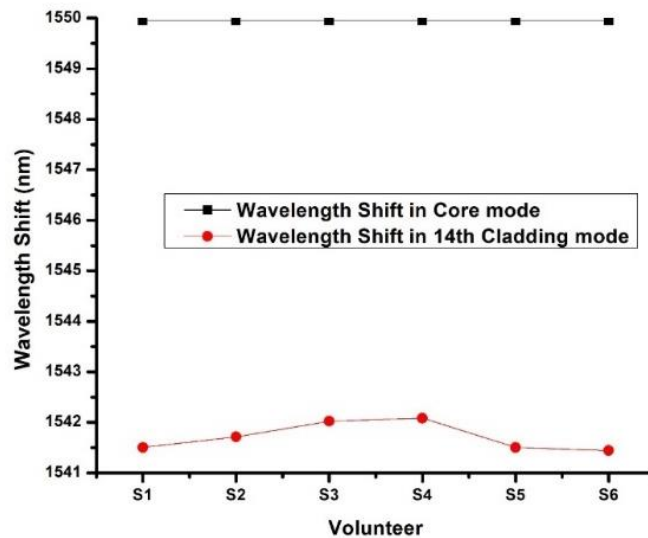


Figure 10. Wavelength shift for core and cladding resonances for six volunteers

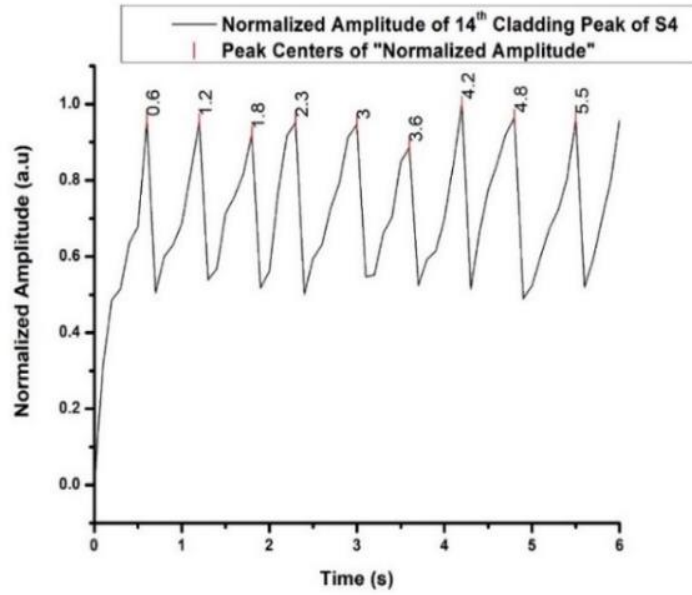


Figure 11. Number of peaks and the time interval between peaks for volunteer S4

Table 3 shows the temperature measurement carried out for six volunteers. Measurement was done for 180 seconds, and the temperature was measured by a reference thermometer every 30 seconds. Table 4 shows heart rate measurements conducted for all volunteers. Measurement was taken for 180 seconds, and validation was done with a reference heart rate monitor for every 90 seconds. An average accuracy of 99.68% and 98.42 % was achieved in temperature and heart rate measurements by the proposed TFBG sensor.

Table 5 summarizes all temperature and heart rate measurements for six volunteers, with an error in validation using reference devices. The next highest integer value from the mean was considered for measured heart rate values. The average response time was found to be 3 seconds for the proposed TFBG sensor for both temperature and heart rate measurements.

The comparison of measured sensor and reference values is analyzed using the Bland-Altman plot. Bland Altman states that the reproducibility of the sensor is good if 95% of measured data lies in the ± 1.96 standard deviation range and the method used for measuring is acceptable in medical practices. Figure 12 shows the Bland Altman plot analysis for temperature as shown in Figure 12(a) and heart rate as shown in Figure 12(b). From the figure, it is observed that the proposed method of simultaneous measurement of vital signs using TFBG can be extended to real-time implementation. Table 6 lists the major findings of the proposed TFBG sensor compared with the FBG sensor. The real-time investigation was carried out in ideal conditions and variations may be found in real-world scenarios.

Table 3. Temperature measurement of volunteers

Volunteer	Temperature readings (°C)	Time (s)							Relative error (%) $\left \frac{T_{Reference} - T_{Measured}}{T_{Measured}} \right \times 100$	Accuracy (%) (100-error)
		30	60	90	120	150	180	Mean		
S1	Reference	36.2	36.2	36.3	36.3	36.3	36.3	36.3	0.27	99.73
	Measured	36.2	36.2	36.3	36.2	36.3	36.2	36.2		
S2	Reference	36	36.1	36.2	36.2	36.2	36.2	36.2	0	100
	Measured	36.2	36.3	36.1	36.2	36.2	36.2	36.2		
S3	Reference	36.3	36.3	36.3	36.3	36.3	36.3	36.3	0.27	99.73
	Measured	36	36.2	36.2	36.2	36.2	36.2	36.2		
S4	Reference	36.1	36.1	36	36	36	36	36.0	0.55	99.45
	Measured	35.8	35.7	35.8	35.8	35.8	35.8	35.8		
S5	Reference	36.3	36.2	36.2	36.2	36.2	36.2	36.2	0.27	99.73
	Measured	36.2	36.2	36.3	36.3	36.3	36.3	36.3		
S6	Reference	36.4	36.2	36.3	36.3	36.3	36.3	36.3	0.54	99.46
	Measured	36.5	36.4	36.5	36.5	36.5	36.5	36.5		
Average accuracy									99.68	

Table 4. Heart rate measurement of volunteers

Volunteer	Heart rate readings (bpm)	Time (s)		Mean	Relative error (%) $\left \frac{H_{Reference} - H_{Measured}}{H_{Measured}} \right \times 100$	Accuracy (%) (100-Error)
		90	180			
S1	Reference	82	81	81.5	1.87	98.13
	Measured	80	80	80		
S2	Reference	89	89	89	1.11	98.89
	Measured	90	90	90		
S3	Reference	99	100	99.5	0.5	99.5
	Measured	100	100	100		
S4	Reference	102	102	102	0.99	99.01
	Measured	101	101	101		
S5	Reference	81	82	81.5	3.16	96.84
	Measured	79	79	79		
S6	Reference	79	80	79.5	1.85	98.15
	Measured	81	81	81		
Average accuracy						98.42

Table 5. Summary of temperature and heart rate measurement of volunteers

Volunteer	Reference temperature (°C)	Reference heart rate (bpm)	Measured temperature (°C)	Measured heart rate (bpm)	Error in temperature (°C)	Error in heart rate (bpm)
S1	36.3	82	36.2	80	0.1	2
S2	36.2	89	36.2	90	0	1
S3	36.3	100	36.2	100	0.1	0
S4	36.0	102	35.8	101	0.2	1
S5	36.2	82	36.3	79	0.1	3
S6	36.3	80	36.5	81	0.2	1

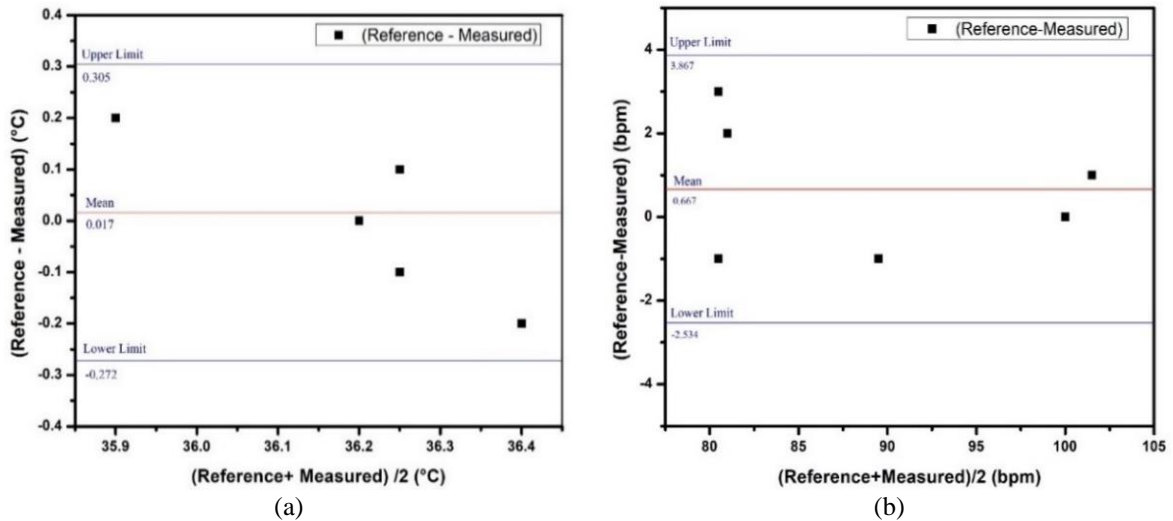


Figure 12. Bland Altman plot for (a) temperature and (b) heart rate measurements

Table 6. Major findings of the study

Parameters	FBG	TFBG
Temperature sensitivity	12 pm/°C	11.81 pm/°C
Strain sensitivity	1.2 pm/με	1.73 pm/με
Simultaneous measurement	NA	11.2 pm/°C, 28.62 pm per heartbeat
Accuracy	96%	98.5%

5. CONCLUSION

Continuous and simultaneous monitoring of various vital signals using a single sensor is an essential stumbling block that needs to be addressed. The proposed TFBG-based optical fiber sensor acts as a solution for that, which enables simultaneous temperature and heart rate measurement based on the wavelength shift in the core and cladding mode resonances. The proposed TFBG-based optical sensor has a sensitivity of

11.81 pm/°C and 1.73 pm/με toward changes in temperature and strain respectively. The average response time was determined to be 3 seconds, and the temperature and heart rate measurements yielded average accuracy of 99.68% and 98.52%, respectively, evincing the accuracy of the sensor. Proposed sensor measurements are analyzed using Bland Altman statistics and found to be acceptable practices that can be implemented for real-time monitoring. Future enhancement can be done by implementing machine learning in the automatic detection of wavelength shifts, making it possible to function as a prototype.

ACKNOWLEDGEMENTS

The authors would like to thank “Apex Telecom Testing Lab” located in Oragadam, Kanchipuram district, Tamil Nadu, India-603109 for permitting to use testing chamber to characterize the sensitivity of TFBG.




REFERENCES

- [1] M. J. Nicolas, R. W. Sullivan, and W. L. Richards, “Large scale applications using FBG sensors: Determination of in-flight loads and shape of a composite aircraft wing,” *Aerospace*, vol. 3, no. 3, 2016, doi: 10.3390/aerospace3030018.
- [2] A. Othonos, K. Kalli, and G. E. Kohnke, “Fiber Bragg gratings: fundamentals and applications in telecommunications and sensing,” *Physics Today*, vol. 53, no. 5, pp. 61–62, 2000, doi: 10.1063/1.883086.
- [3] X. Li, M. Zheng, D. Hou, and Q. Wen, “Advantageous strain sensing performances of FBG strain sensors equipped with planar UV-Curable resin,” *Sensors*, vol. 23, no. 5, 2023, doi: 10.3390/s23052811.
- [4] A. Ferreira Da Silva *et al.*, “A smart skin PVC foil based on FBG sensors for monitoring strain and temperature,” *IEEE Transactions on Industrial Electronics*, vol. 58, no. 7, pp. 2728–2735, 2011, doi: 10.1109/TIE.2010.2057233.
- [5] P. Orr and P. Niewczasz, “High-speed, solid state, interferometric interrogator and multiplexer for fiber Bragg grating sensors,” *Journal of Lightwave Technology*, vol. 29, no. 22, pp. 3387–3392, 2011, doi: 10.1109/JLT.2011.2169044.
- [6] M. M. Keshk, I. A. Ashry, M. H. Aly, and A. M. Okaz, “Analysis of different fiber Bragg gratings for use in a multi-wavelength erbium doped fiber laser,” *National Radio Science Conference, NRSC, Proceedings*, 2007, doi: 10.1109/NRSC.2007.371409.
- [7] J. Braunfelds *et al.*, “FBG-based sensing for structural health monitoring of road infrastructure,” *Journal of Sensors*, vol. 2021, 2021, doi: 10.1155/2021/8850368.
- [8] I. Sousa *et al.*, “Sensing system based on FBG for corrosion monitoring in metallic structures,” *Sensors*, vol. 22, no. 16, 2022, doi: 10.3390/s22165947.
- [9] J.-B. Lecourt, C. Duterte, F. Narbonneau, D. Kinet, Y. Hernandez, and D. Giannone, “All-normal dispersion, all-fibered PM laser mode-locked by SESAM,” *Optics Express*, vol. 20, no. 11, p. 11918, 2012, doi: 10.1364/oe.20.011918.
- [10] J. Nedoma, M. Fajkus, P. Siska, R. Martinek, and V. Vasinek, “Non-invasive fiber optic probe encapsulated into PolyDiMethylSiloxane for measuring respiratory and heart rate of the human body,” *Advances in Electrical and Electronic Engineering*, vol. 15, no. 1, pp. 93–100, 2017, doi: 10.15598/aeec.v15i1.1923.
- [11] M. Fajkus, J. Nedoma, R. Martinek, V. Vasinek, H. Nazeran, and P. Siska, “A non-invasive multichannel hybrid fiber-optic sensor system for vital sign monitoring,” *Sensors (Switzerland)*, vol. 17, no. 1, 2017, doi: 10.3390/s17010111.
- [12] A. Manujlo and T. Osuch, “Temperature fiber Bragg grating based sensor for respiration monitoring,” *Photonics Applications in Astronomy, Communications, Industry, and High Energy Physics Experiments 2017*, vol. 10445, p. 104451A, 2017, doi: 10.1117/12.2281106.
- [13] A. H. Ali, A. I. Mahmood, M. A. Hussien, M. J. Ali, A. I. Mahmood, and M. A. Hussien, “Human body high resolution and accurate temperature FBG sensor,” *IOP Conference Series: Earth and Environmental Science*, vol. 779, no. 1, 2021, doi: 10.1088/1755-1315/779/1/012029.
- [14] P. B. Prathap and K. Saara, “Fiber Bragg grating as a temperature sensor for human body temperature monitoring,” *Journal of Optics (India)*, 2024, doi: 10.1007/s12596-024-01894-y.
- [15] K. Chethana, A. S. G. Prasad, S. N. Omkar, and S. Asokan, “Fiber Bragg grating sensor based device for simultaneous measurement of respiratory and cardiac activities,” *Journal of Biophotonics*, vol. 10, no. 2, pp. 278–285, 2017, doi: 10.1002/jbio.201500268.
- [16] J. Nedoma, M. Fajkus, R. Martinek, and H. Nazeran, “Vital sign monitoring and cardiac triggering at 1.5 tesla: A practical solution by an mr-ballistocardiography fiber-optic sensor,” *Sensors (Switzerland)*, vol. 19, no. 3, 2019, doi: 10.3390/s19030470.
- [17] J. Nedoma, M. Fajkus, R. Martinek, and V. Vasinek, “Non-invasive fiber-optic biomedical sensor for basic vital sign monitoring,” *Advances in Electrical and Electronic Engineering*, vol. 15, no. 2, pp. 336–342, 2017, doi: 10.15598/aeec.v15i2.2131.
- [18] M. Krej, L. Dziuda, and F. W. Skibniewski, “A method of detecting heartbeat locations in the ballistocardiographic signal from the fiber-optic vital signs sensor,” *IEEE Journal of Biomedical and Health Informatics*, vol. 19, no. 4, pp. 1443–1450, 2015, doi: 10.1109/JBHI.2015.2392796.
- [19] S. Kurasawa, S. Koyama, H. Ishizawa, K. Fujimoto, and S. Chino, “Verification of non-invasive blood glucose measurement method based on pulse wave signal detected by FBG sensor system,” *Sensors (Switzerland)*, vol. 17, no. 12, 2017, doi: 10.3390/s17122702.
- [20] J. Bonafacino *et al.*, “Ultra-fast polymer optical fibre Bragg grating inscription for medical devices,” *Light: Science and Applications*, vol. 7, no. 3, p. 17161, 2018, doi: 10.1038/lsa.2017.161.
- [21] W. Chen *et al.*, “Helical long period fiber grating sensor for non-invasive measurement of vital signs,” *Optics and Laser Technology*, vol. 162, 2023, doi: 10.1016/j.optlastec.2023.109293.
- [22] K. Krebber, S. Liehr, and J. Witt, “Smart technical textiles based on fibre optic sensors,” *OFS2012 22nd International Conference on Optical Fiber Sensors*, vol. 8421, pp. 84212A–84212A–10, 2012, doi: 10.1117/12.981342.
- [23] T. Elsamagawy, J. Hauelsen, M. Farrag, S. G. Ansari, and H. Fouad, “Embedded fiber Bragg grating based strain sensor as smart costume for vital signal sensing,” *Sensor Letters*, vol. 12, no. 11, pp. 1669–1674, 2014, doi: 10.1166/sl.2014.3382.
- [24] R. Arumugam, R. Kumar, S. Dhanalakshmi, K. Wee Lai, L. Jiao, and X. Wu, “Novel apodized fiber Bragg grating applied for medical sensors: performance investigation,” *Computer Modeling in Engineering & Sciences*, vol. 135, no. 1, pp. 301–323, 2023, doi: 10.32604/cmescs.2022.022144.
- [25] R. Arumugam, R. Kumar, and S. Dhanalakshmi, “Optimization and performance evaluation of apodization function for fiber Bragg grating as vital sign sensor,” *IFMBE Proceedings*, vol. 86, pp. 341–350, 2022, doi: 10.1007/978-3-030-90724-2_37.




- [26] Y. Koyama, M. Nishiyama, and K. Watanabe, "Smart textile using hetero-core optical fiber for heartbeat and respiration monitoring," *IEEE Sensors Journal*, vol. 18, no. 15, pp. 6175–6180, 2018, doi: 10.1109/JSEN.2018.2847333.
- [27] J. Yu, S. Xu, Y. Jiang, H. Chen, and W. Feng, "Multi-parameter sensor based on the fiber Bragg grating combined with triangular-lattice four-core fiber," *Optik*, vol. 208, 2020, doi: 10.1016/j.ijleo.2019.164094.
- [28] A. Urrutia, J. Goicoechea, A. L. Ricchiuti, D. Barrera, S. Sales, and F. J. Arregui, "Simultaneous measurement of humidity and temperature based on a partially coated optical fiber long period grating," *Sensors and Actuators, B: Chemical*, vol. 227, pp. 135–141, 2016, doi: 10.1016/j.snb.2015.12.031.
- [29] T. Geng *et al.*, "A temperature-insensitive refractive index sensor based on no-core fiber embedded long period grating," *Journal of Lightwave Technology*, vol. 35, no. 24, pp. 5391–5396, 2017, doi: 10.1109/JLT.2017.2772304.
- [30] Q. Yu, Y. Zhang, Y. Dong, Y. P. Li, C. Wang, and H. Chen, "Study on optical fiber Bragg grating temperature sensors for human body temperature monitoring," *2012 Symposium on Photonics and Optoelectronics, SOPO 2012*, 2012, doi: 10.1109/SOPO.2012.6271111.
- [31] R. Arumugam, K. Ramamoorthy, and D. Samiappan, "Study of various structures of Bragg fibers based on modal analysis," *Springer Proceedings in Physics*, vol. 258, pp. 271–274, 2021, doi: 10.1007/978-981-15-9259-1_62.
- [32] J. Albert, L. Y. Shao, and C. Caucheteur, "Tilted fiber Bragg grating sensors," *Laser and Photonics Reviews*, vol. 7, no. 1, pp. 83–108, 2013, doi: 10.1002/lpor.201100039.
- [33] C. Chen, L. Xiong, A. Jafari, and J. Albert, "Differential sensitivity characteristics of tilted fiber Bragg grating sensors," *Fiber Optic Sensor Technology and Applications IV*, vol. 6004, p. 60040B, 2005, doi: 10.1117/12.629975.
- [34] S. E. Kipriksiz and M. Yücel, "Tilted fiber Bragg grating design for a simultaneous measurement of temperature and strain," *Optical and Quantum Electronics*, vol. 53, no. 1, 2021, doi: 10.1007/s11082-020-02609-w.

BIOGRAPHIES OF AUTHORS






Ramya Arumugam    received her master's degree in applied electronics from College of Engineering, Anna University, Chennai in 2012 and Bachelor's degree from Madha Engineering College, Chennai in 2009. She has 11+ years of academic experience. Currently she is working as assistant professor in the Department of Electronics and Communication Engineering, SRM Institute of Science and Technology, Chennai, India. Her areas of interest optical sensor, fiber Bragg grating, machine learning and signal processing. She can be contacted at email: ramyaa@srmist.edu.in.



Ramamoorthy Kumar    received his Ph.D. degree from SRM University, India (2009), Master of Science from BITS Pilani (1993) bachelors' degree in electronics and communication engineering from Bharathidasan University, Tamil Nadu, India (1989). He is working as a professor in the Department of Electronics and Communication Engineering, SRM University, Chennai, India. His areas of interest include spread spectrum techniques, wireless communication, cognitive radio, wireless sensor networks and MIMO-OFDM systems. He has supervised several undergraduate, postgraduate as well as Ph.D. students in the area of wireless communication. He has published more than 60 papers in international conferences and journals. He may be contacted at email: kumarr@srmist.edu.in.



Samiappan Dhanalakshmi    received the BE degree in electrical and electronics engineering from Bharathiyar University with the "Overall Best Outgoing Student Award" at Kongu Engineering College in 2002. She received an M.E. Degree in applied electronics with a Silver Medal from Anna University in 2004 and a Ph.D. in information and communication engineering from Anna University Chennai in 2014. With more than 19 + years of academic and research experience, she is presently a professor with the Department of Electronics and Communication Engineering at SRM Institute of Science and Technology, Kattankulathur, where she is heading the Underwater Optical Sensors R&D Laboratory. She has authored 200+ technical papers in SCI/Scopus Indexed journals. Her research interests include FBG sensing, machine learning, signal, speech and image processing. She has organized National-level workshops, seminars, and FDPs funded by DRDO, AICTE, ICMR, IEL, and CFD Anna University. She has delivered over 20 guest lecturers for faculty and students at a few engineering colleges. She is the principal investigator of four projects and the principal guide for several other projects. She has published five patents to her credit. She was awarded the "Dr.A.P.J. Abdul Kalam Inspiring Teacher Award", by IET CLN in 2016 and was also Awarded the "Best Woman Engineer Award" by Inst. of Engineers, Tamilnadu in 2019. She was recognized as the founder and honorary secretary for the Institution of Engineers, Kattankulathur Local Centre, in December 2019. She is a fellow member of IE(I) and IETE and a life member of the optical society of India. She may be contacted at email: dhanalas@srmist.edu.in.